A Preliminary Investigation of the Additivity of $\pi-\pi$ or $\pi^+-\pi$ Stacking and T-Shaped Interactions between Natural or Damaged DNA Nucleobases and Histidine

Lesley R. Rutledge, Cassandra D. M. Churchill, and Stacey D. Wetmore*

Department of Chemistry and Biochemistry, University of Lethbridge, 4401 University Drive, Lethbridge, Alberta T1K 3M4, Canada

Received: December 18, 2009; Revised Manuscript Received: January 21, 2010

Previous computational studies have examined $\pi-\pi$ and $\pi^+-\pi$ stacking and T-shaped interactions in nucleobase−amino acid dimers, yet it is important to investigate how additional amino acids affect these interactions since simultaneous contacts often appear in nature. Therefore, this paper investigates the geometries and binding strengths of amino acid−nucleobase−amino acid trimers, which are compared to the corresponding nucleobase−amino acid dimer interactions. We concentrate on systems containing the natural nucleobase adenine or its (cationic) damaged counterpart, 3-methyladenine, and the aromatic amino acid histidine, in both the neutral and protonated forms. This choice of molecules provides information about $\pi-\pi$ and $\pi^+-\pi$ stacking and T-shaped interactions in asymmetric, biologically relevant systems. We determined that both stacked and T-shaped interactions, as well as both $\pi-\pi$ and $\pi^+-\pi$ interactions, exhibit geometric additivity. To investigate the energetic additivity in our trimers, the synergy (E_{syn}) and the additivity (E_{add}) energy were examined. E_{add} reveals that it is important to consider the interaction between the two amino acids when examining the additivity of nucleobase−amino acid interactions. Additionally, E_{syn} and E_{add} indicate that $\pi^+-\pi$ interactions are quite different from $\pi-\pi$ interactions. The magnitude of E_{add} is generally less than 2 kJ mol^{-1}, which suggests that these interactions are additive. However, the interaction energy analysis does not provide information about the individual interactions in the trimers. Therefore, the quantum theory of atoms in molecules (QTAIM) was implemented. We find inconsistent conclusions from our QTAIM analysis and interaction energy evaluation. However, the magnitudes of the differences between the dimer and trimer critical point properties are extremely small and therefore may not be able to yield conclusive descriptions of differences (if any) between the dimer and trimer interactions. We hypothesize that, due to the limited number of investigations of this type, it is currently unclear how QTAIM can improve our understanding of $\pi-\pi$ and $\pi^+-\pi$ dimers and trimers. Therefore, future work must systematically alter the $\pi-\pi$ or $\pi^+-\pi$ system to definitively determine how the geometry, symmetry, and system size alter the QTAIM analysis, which can then be used to understand biologically relevant complexes.

1. Introduction

Noncovalent interactions are pivotal in regulating biochemical processes that occur at DNA−protein interfaces. For example, DNA−protein interactions are very important in DNA repair, where nucleobase−amino acid contacts are crucial for the identification and selective removal of damaged bases.[1−3] In the most common DNA repair pathway, the base excision repair (BER) mechanism,[3] multiple enzymes work together to identify damaged nucleobases and leave the natural bases intact. The first enzyme in the BER mechanism, the DNA glycosylase, recognizes a specific type of damaged nucleobase, flips the corresponding nucleotide out of the DNA helix and into the active site, and cleaves the glycosidic bond connecting the nucleobase to the sugar−phosphate backbone.[1,2] The DNA glycosylases use a variety of noncovalent interactions (such as hydrogen bonding, $\pi-\pi$ stacking, and X−H$\cdots\pi$ (X = N, C, O, S) and/or $\pi-\pi$ T-shaped) to recognize, bind, and facilitate excision of the damaged base.[1,2] Additionally, when the DNA glycosylase flips the target base out of DNA, a conjugated amino acid is commonly inserted into the DNA helix to stabilize the distorted DNA strand through $\pi-\pi$ stacking interactions.[1,2]

To understand how aromatic amino acids interact with natural or damaged nucleobases in DNA−protein complexes, a variety of experimental crystal structures have been analyzed for these contacts.[4,5] Approximately one-third of these direct contacts are specific hydrogen bonds between DNA base pairs and amino acid side chains, and the nature of these interactions has been widely studied. Conversely, the remaining interactions (such as $\pi-\pi$ (face-to-face) stacking and $\pi-\pi$ (edge-to-face) T-shaped) are not as well understood, yet can play a significant role in the overall stability of DNA−protein complexes. Computational chemistry can provide valuable information about the preferred structures and relative magnitudes, as well as the structure−magnitude relationship of these noncovalent interactions.

Accurate ab initio techniques have been used to study the $\pi-\pi$ stacking and $\pi-\pi$ T-shaped interactions between the natural nucleobases and the aromatic amino acids. The Hu group,[6] as well as the Tschumper group,[7] have considered adenine stacked with a variety of amino acids in orientations found in experimental crystal structures. The Rooman group has also investigated stacking and T-shaped orientations of adenine and phenylalanine or histidine (neutral and protonated) found in crystal structures, as well as optimal geometries identified through potential energy surface scans.[8] Optimized

* Corresponding author. Tel: +1 403 329 2323. Fax: +1 402 329 2057. E-mail: stacey.wetmore@uleth.ca.

10.1021/jp911990g
Published on Web 02/12/2010

stacked geometries between the aromatic amino acids and cytosine or uracil have also been examined by Cysewski,[9] and the (constrained) optimized uracil−phenylalanine stacked dimer has recently been investigated by Ebrahimi and co-workers.[10]

Our lab has extensively characterized the stacking interactions between the four aromatic amino acids and natural[11] or damaged[12] nucleobases through detailed potential energy surface scans. Furthermore, our group has investigated the $\pi-\pi$ (edge-to-face) T-shaped interactions between the natural nucleobases and the four aromatic amino acids.[13] Due to the unique pK_a of histidine, which allows for neutral or protonated forms at physiological conditions,[8] our most recent study considered the stacking and T-shaped interactions between protonated histidine and the natural nucleobases.[14] In addition to natural bases, we have investigated the T-shaped interactions between the aromatic amino acids and 3-methyladenine[15] since this base stops replication and therefore is arguably one of the most detrimental forms of DNA alkylation damage.[16] Our technique for characterizing the potential energy surfaces of these dimers has allowed us to clarify the dependence of stacking and T-shaped interactions on various geometric variables, as well as identify optimal dimer orientations. Furthermore, our scans provide information about how the relative orientations of monomers affect the strength of each interaction, and our data set can be used by biochemists to accurately approximate the magnitude and relative importance of experimentally observed π-interactions in DNA−protein complexes.[13]

It is important to study dimers to develop our understanding of nucleobase−amino acid contacts. However, more than one noncovalent interaction can occur simultaneously in nature. For example, in the human alkyladenine DNA glycosylase (AAG), which removes 3-methyladenine and other alkylated purines from DNA,[1,2] multiple stacking and T-shaped interactions are exploited to bind substrates in the active site.[17] Therefore, it is important to investigate how additional amino acids affect the $\pi-\pi$ interactions in nucleobase−amino acid dimers. In fact, both the geometry and binding energy of a dimer may be affected by additional contacts. Alternatively, it is possible that the monomers in the trimer retain their preferred relative orientations in the dimer (geometric additivity) and the resulting interactions between monomers are of equal strength in the dimer and trimer (energetic additivity).

Previous computational studies have examined the geometric and energetic additivity of a variety of noncovalent interactions (such as hydrogen bonding, $\pi-\pi$ stacking, $\pi-\pi$ T-shaped, small molecule X−H$\cdots\pi$ (X = N, C, O, S) T-shaped, cation−π (involving a cationic point charge), and $\pi^+-\pi$ (involving a cationic π-system)) in biological and nonbiological systems (for select studies see refs 10 and 18−39). For example, extensive studies have been conducted on the $\pi-\pi$ stacking and $\pi-\pi$ T-shaped interactions between benzene rings in trimers and tetramers.[18−20] DNA nucleobase trimers have also been investigated to understand the additivity of stacking and hydrogen-bonding interactions.[21−23,37] A recent study investigated the additivity of $\pi-\pi$ stacking and $Na^+-\pi$ interactions in trimers composed of uracil, phenylalanine, and sodium ions.[10] Furthermore, a large number of calculations have recently been conducted by Frontera et al. that study the interplay between a wide range of noncovalent interactions involving various molecular systems.[26−31,34−36]

Despite the significant number of complexes studied in the literature, very few groups have considered the geometry and binding strength of (edge-to-face) T-shaped interactions between π-ring systems in trimers.[18,19,25−27,29,32] Additionally, complexes

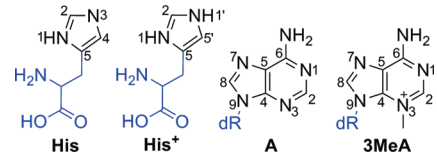

Figure 1. Structure and atomic numbering of the aromatic amino acid (histidine (HIS) and protonated histidine (HIS^+)) and nucleobases (adenine (A) and 3-methyladenine (3MeA)) considered in this study. Blue fragments were replaced with a hydrogen atom in our models.

previously investigated involve symmetric molecules, which result in highly symmetric trimers.[18,19,26,27,29,32] To the best of our knowledge, only one study considered $\pi-\pi$ T-shaped interactions in asymmetric (C_1) trimers other than benzene trimers.[25] Although the effects of hydrogen bonding a small molecule (H_2O, Cl^-, or Br^-) to a T-shaped interaction were considered in trimers,[25] the additivity of T-shaped contacts with other $\pi-\pi$ contacts was not studied. Therefore, in order to truly understand the interplay between $\pi-\pi$ stacking and $\pi-\pi$ T-shaped interactions in biological systems (such as those in the active site of AAG), trimers involving many relative arrangements of the nucleobases and the aromatic amino acids must be investigated.

To complement geometric and energetic information for trimers, some researchers have used Bader's quantum theory of atoms in molecules (QTAIM)[40−43] analysis. QTAIM has been widely used to characterize a large assortment of noncovalent interactions (for examples, see refs 10, 26−32, 34, 38, 39, and 44−65), and may be quite powerful for analyzing the cooperative effects of the interactions within trimers. However, QTAIM analysis for $\pi-\pi$ and $\pi^+-\pi$ stacked and T-shaped systems is scarce in the literature, and few studies have examined systems with C_1 symmetry and/or biologically relevant molecules.[10,20,44,49,50,52−54,59]

This paper investigates the geometries and binding strengths of amino acid−nucleobase−amino acid trimers, which will be compared to the corresponding dimers previously studied by our group.[13−15] As a test case, we concentrated on systems containing the natural nucleobase adenine (A) or its (cationic) damaged counterpart, 3-methyladenine (3MeA), and the aromatic amino acid histidine, in both the neutral (His) and protonated (His^+) forms (Figure 1). This study will provide information about the geometric and energetic additivity of $\pi-\pi$ stacking and $\pi-\pi$ T-shaped interactions in asymmetric systems. Additionally, this paper will reveal differences in the additivity and interplay of (neutral) $\pi-\pi$ and (cationic) $\pi^+-\pi$ interactions by introducing the cationic charge in the central nucleobase (3MeA) or the terminal amino acid (His^+). Recent work[25] suggests that the poorly understood $\pi^+-\pi$ interactions are quite different from the typically examined cation−π interactions involving a cationic point charge, where it has been proposed that cation−π interactions strengthen in trimers and result in a greater than additive interaction energy.[10,24,28,31,34−36] Finally, this paper will use QTAIM to analyze the interaction energies in nucleobase−amino acid dimers and trimers to help bridge the gap in the current QTAIM literature.

2. Computational Details

2.1. Geometries of Dimers. Previous work in our laboratory[11−15] used a series of counterpoise-corrected[66] MP2/6-31G*(0.25) single-point calculations to scan the potential energy surface for the stacked and T-shaped orientations of nucleobase−amino acid dimers. Several geometric variables were considered (Figure 2), which is similar to the approach used by Hobza and

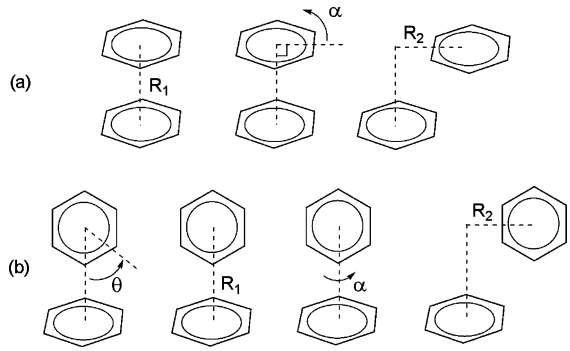

Figure 2. Definition of the variables considered in previous (a) $\pi-\pi$ and $\pi^+-\pi$ stacking potential energy surface scans (vertical separation (R_1), angle of rotation (α), and horizontal displacement (R_2)), and (b) $\pi-\pi$ and $\pi^+-\pi$ T-shaped potential energy surface scans (angle of "edge" rotation, (θ), vertical separation (R_1), angle of rotation (α), and horizontal displacement (R_2)).[13−15]

Šponer to study the natural nucleobase dimers.[67−69] As mentioned in the Introduction, this method for scanning the potential energy surface provides more information than simply the optimal stacking and T-shaped geometries. Specifically, our scans also provide a structure−magnitude relationship that can be used to characterize DNA−protein active sites identified through experiment.[13] Additionally, MP2/6-31G*(0.25) was chosen due to its computational efficiency for the large number of points considered and it has been shown to have remarkable agreement with CCSD(T)/CBS interaction energies for the nucleobase−amino acid dimers discussed in this study.[13−15]

To determine the preferred dimer geometries, C_s symmetric, MP2/6-31G(d) optimized monomers (Figure 1) were placed so that the nucleobase and amino acid molecular planes were parallel (stacked) or perpendicular (T-shaped). In the case of His, two molecular planes were considered. The first was obtained by stacking His on top of the nucleobase in the orientation shown in Figure 1 (denoted as HIS). The second was obtained by mirror flipping His relative to Figure 1 before stacking with the nucleobase (denoted as HIS′). T-shaped dimers involving His or His^+ edges (denoted as HIS(edge) or HIS^+(edge), respectively) were also previously considered.[13−15] To define the His or His^+ edge directed at the nucleobase π-system, the geometric variable θ (Figure 2b) was introduced. We considered atom directed edges (an atom of His or His^+ directed toward the center of mass of the nucleobase), as well as bridged edges (more than one atom directed toward the center of mass of the nucleobase).

From these initial structures, three geometric variables (Figure 2: vertical separation (R_1), angle of rotation (α), and horizontal displacement (R_2)) were considered in our MP2/6-31G*(0.25) potential energy surface scans. First, R_1 was altered by 0.1 Å increments. Second, at the preferred R_1 separation, an α-scan was performed in 30° increments by rotating His or His^+ in a right-hand sense relative to the nucleobase. Finally, at the preferred R_1 and α, R_2 was considered by shifting His or His^+ relative to the nucleobase in 0.5 Å increments across a grid. Specifically, the center of mass of the nucleobase was set to the origin (0 Å, 0 Å), and His or His^+ was shifted in two horizontal directions (perpendicular to the R_1 vertical separation axis). Full details on the edges considered, and our scan procedure, are provided in our previous manuscripts.[13−15]

2.2. Geometries of Trimers. In the present study, we investigated trimers composed of one amino acid located directly above, and a second amino acid directly below the molecular plane of the nucleobase. All combinations of stacked and T-shaped orientations were considered to yield three possible trimer arrangements: (1) stacked_stacked, (2) stacked_T-shaped, and (3) T-shaped_T-shaped. To distinguish between the geometries and molecules examined, each trimer is named according to its corresponding dimers. For example, in the HIS_A_HIS(edge) trimer, one histidine is stacked (HIS) with adenine, which is the central monomer, and another histidine is T-shaped (HIS(edge)) relative to adenine. Due to our choice of molecules and differences in their total charges, we considered three types of trimers: A and two neutral His (His:A:His), cationic 3MeA and two neutral His (His:3MeA:His), and A with one neutral His and one charged His^+ (His:A:His^+). In the case of T-shaped trimers, only the optimal amino acid edge previously identified for the dimers was considered.[13−15] This combination of stacked (HIS, HIS′, or HIS^+) or T-shaped (HIS(edge) or HIS^+(edge)) orientations yields 18 trimers (six His:A:His, six His:3MeA:His, and six His:A:His^+). It should be noted that because the nucleobases are fixed in planar C_s symmetry, it does not matter whether the interaction occurs "above" or "below" the plane of the nucleobase.

MP2/6-31G*(0.25) potential energy surface scans were performed for six representative trimers to determine how the preferred trimer geometry differs from the preferred dimer geometries. This choice in trimers will allow us to understand the interplay between two $\pi-\pi$ or two $\pi^+-\pi$ interactions, which are specific to our intended application (DNA repair). We also expect these trimers to exhibit the largest geometrical changes relative to the dimers. Specifically, for the HIS_A_HIS, HIS_A_HIS(edge), HIS(edge)_A_HIS(edge), HIS′_3MeA_HIS′, HIS′_3MeA_HIS(edge), and HIS(edge)_3MeA_HIS(edge) trimers, the monomers were first aligned according to their centers of mass. Next, an R_1 scan was performed for one amino acid in 0.1 Å increments. At each of these R_1 values, a full R_1 scan was completed for the second amino acid. Once the lowest energy structure was identified, the preferred R_1 distances were held constant and the preferred α values were determined. Specifically, for every 30° rotation of one amino acid, a full α-scan was completed for the other amino acid, and vice versa. Once the best α values were determined for both amino acids, R_2 scans were performed simultaneously on the area surrounding the dimer global minima. This procedure resulted in over 950 points scanned for each trimer.

2.3. Interaction Energy of Trimers. For each amino acid−nucleobase dimer and amino acid−nucleobase−amino acid trimer, the interaction energies (ΔE_{dimer} and ΔE_{trimer}, respectively) were evaluated as follows:

$$\Delta E_{dimer} = E_{12} - E_1 - E_2 \quad (1)$$

$$\Delta E_{trimer} = E_{123} - E_1 - E_2 - E_3 \quad (2)$$

where E_{12} (E_{123}) is the MP2/6-31G*(0.25) energy of the dimer (trimer) which includes a basis set superposition error (BSSE) correction calculated according to the counterpoise method.[66] E_1 and E_3 are the amino acid monomer energies, and E_2 is the nucleobase monomer energy.

To further evaluate the interplay of stacking and T-shaped interactions in trimers, two quantities denoted as E_{syn} (synergy energy) and E_{add} (additivity energy) were calculated as follows:

$$E_{syn} = \Delta E_{trimer(123)} - \Delta E_{dimer(12)} - \Delta E_{dimer(23)} \quad (3)$$

$$E_{add} = \Delta E_{trimer(123)} - \Delta E_{dimer(12)} - \Delta E_{dimer(23)} - \Delta E_{dimer(13)} \quad (4)$$

The MP2/6-31G*(0.25) synergy energy (E_{syn}) is the difference between the trimer interaction energy and the two nucleobase−amino acid dimer interaction energies ($\Delta E_{dimer(12)}$ and $\Delta E_{dimer(23)}$). The MP2/6-31G*(0.25) additivity energy is the difference between the trimer interaction energy and the sum of all pairwise interaction energies ($\Delta E_{dimer(12)}$, $\Delta E_{dimer(23)}$, and $\Delta E_{dimer(13)}$). All pairwise interactions were calculated according to eq 1.

All trimer potential energy surface scans and interaction energy calculations were completed with Gaussian 03.[70] To further investigate the synergy and additivity of these noncovalent interactions, MP2/6-31G*(0.25) electron densities for dimers and trimers were generated with Gaussian 09,[71] and analyzed according to the quantum theory of atoms in molecules (QTAIM).[40−42] Explicitly, AIMAll[72] was used for electron density critical point analysis and the AIM2000[73] program was used to generate molecular graphs. All reported interaction energies correspond to (BSSE-free) counterpoise-corrected[66] MP2/6-31G*(0.25).

3. Results and Discussion

3.1. Geometric Additivity in Trimers. As mentioned in the Computational Details, it is important to determine whether the geometries of the nucleobase−amino acid dimers change upon inclusion of an additional amino acid in the trimer. To determine the preferred trimer geometries, six test cases were considered and potential energy surface scans of both amino acids in these trimers were completed simultaneously. For five of the six trimers (HIS_A_HIS, HIS_A_HIS(edge), HIS(edge)_A_HIS-(edge), HIS′_3MeA_HIS(edge), HIS(edge)_3MeA_HIS(edge)), all preferred R_1 and α values for the trimer match the optimal geometric parameters for the respective dimers previously determined by our group (see Supporting Information (Table SI-1) for the HIS_A_HIS(edge) example). Additionally, R_2 scans were performed on points surrounding the dimer global minima and revealed that the trimer R_2 minima occur at the same point on the potential energy surface as the corresponding dimer minima (Table SI-1).

In the case of HIS′_3MeA_HIS′, the optimal R_1 and R_2 values for the trimer matched those for the dimer (see Supporting Information (Table SI-2)). However, the preferred α minimum for the histidine and 3-methyladenine dimer (α = 180°) was obtained for one stacked histidine in the trimer, but the other stacked histidine prefers α = 150°. Nevertheless, the 3MeA_HIS′ dimer with α = 180° (−52.3 kJ mol^{-1}) is only 0.1 kJ mol^{-1} more stable than the structure with α = 150°. Since the preferred α value for the trimer and dimer differ by only one (30°) increment, an additional α-scan was performed on the HIS′_3MeA_HIS′ trimer and 3MeA_HIS′ dimer using smaller (3°) increments. In both the dimer and trimer, our more refined search determined the minimum to occur at α = 165° (Table SI-2), where the dimer (trimer) with α = 165° is only 0.7 (1.2) kJ mol^{-1} more stable than the original minimum. Therefore, although the HIS′_3MeA_HIS′ trimer is sensitive to the increments originally used in our potential energy surface scans, the geometries are in fact additive.

Our finding that the preferred trimer geometries match those for the corresponding dimers is consistent with previous work on the benzene (sandwich) trimer.[18] Specifically, the intermolecular separation distance in the benzene trimer is increased by only 0.05 Å relative to the dimer, which results in a total energy change of only 0.1 kJ mol^{-1}. The present study reveals that this geometric additivity holds for both π−π stacked and π−π T-shaped interactions, as well as both π−π and π$^+$−π interactions. Thus, all trimers discussed in the remainder of our study were constructed using the geometric variables previously determined to yield the strongest (most negative) dimer interaction energies.[13−15]

3.2. Interaction Energies of Trimers. The interaction energies computed for the 18 amino acid−nucleobase−amino acid trimers, as well as the corresponding dimers, are summarized in Table 1. An energetic dissection of each trimer energy into the dimer components, as well as the synergy (E_{syn}) and additivity (E_{add}) energy, is also included. To clarify these energetic components, the HIS_A_HIS(edge) trimer is illustrated in Figure 3. In this trimer, one histidine is stacked with A (HIS) and one histidine is T-shaped with A (HIS(edge)). The total counterpoise-corrected binding energy for this three-component system is −52.5 kJ mol^{-1} (Figure 3a). The nearest-neighbor nucleobase−amino acid dimers have interaction energies of −22.5 (HIS(edge), Figure 3b) and −29.7 (HIS, Figure 3c) kJ mol^{-1}, and therefore their sum is −52.2 kJ mol^{-1}. By subtracting the sum of these nucleobase−amino acid dimer energies ($\Delta E_{dimer(12)} + \Delta E_{dimer(23)}$, Table 1) from the total trimer interaction energy, we obtain the synergy energy (E_{syn} = −0.3 kJ mol^{-1}). E_{syn} provides valuable information regarding the interplay between two nucleobase−amino acid interactions, where the slightly negative value for the HIS_A_HIS(edge) trimer indicates that the total binding energy of the trimer is only marginally stronger than the sum of the two nearest-neighbor dimer interactions. Table 1 also reports the interaction energy between the two amino acids when the nucleobase is not present ($\Delta E_{dimer(13)}$). In the HIS_A_HIS(edge) trimer, the histidine−histidine interaction (Figure 3d) is slightly attractive (−0.4 kJ mol^{-1}). The mutual influence of both nucleobase−amino acid interactions is evaluated by including this interaction energy ($E_{add} = E_{syn} - \Delta E_{dimer(13)}$). E_{add} = 0.1 kJ mol^{-1} indicates that the HIS_A_HIS(edge) trimer interaction can be predicted as a sum of the three pairwise binding energies, or that these interactions are additive.

Examination of E_{syn} (Table 1) indicates that trimers involving adenine as the central nucleobase (His:A:His and His:A:His$^+$ complexes) are either strengthened ($E_{syn} < 0$) or weakened ($E_{syn} > 0$) when compared to the two corresponding nucleobase−amino acid dimers. However, the magnitude of E_{syn} is smallest for the neutral His:A:His trimers, suggesting that π−π interactions have different properties from π$^+$−π interactions. For trimers containing 3MeA, E_{syn} is positive, which indicates that the trimer interaction energy is weaker than predicted from the sum of two nucleobase−amino acid dimers. In 3MeA trimers, any given dimer interaction weakens since the cationic charge located on the central monomer becomes delocalized over the entire complex upon trimer formation. These results are consistent with the work by Singh et al.,[25] where weakening of π$^+$−π interactions (methylimidazolium−benzene) in H_2O−π$^+$−π trimers (water molecule hydrogen bonded to methyl imidazolium) was observed. Contrary to 3MeA trimers, the cationic charge in His:A:His$^+$ trimers is localized at one end of the complex, which is similar to previously studied[10,24,28,31,34−36] cation−π trimers involving cationic point charges (such as Li^+ or Na^+). These works report a significant strengthening of the cation−π interaction in the trimer compared to the dimers, which is contrary to our results for π$^+$−π trimers involving His$^+$ ($E_{syn} > 0$, Table 1). Therefore, our results support the conclusions of Singh et al.[25] that π$^+$−π interactions are a special type of π-interaction with features unique from cation−π

TABLE 1: MP2/6-31G*(0.25) Total Dimer and Trimer Interaction Energies, as Well as Synergy (E_{syn}) and Additivity (E_{add}) Energies for the Trimers (kJ mol^{-1})

complex	ΔE^a	$\Delta E_{dimer(12)} + \Delta E_{dimer(23)}{}^b$	$E_{syn}{}^c$	$\Delta E_{dimer(13)}{}^d$	$\Delta E_{dimer(12)} + \Delta E_{dimer(23)} + \Delta E_{dimer(13)}{}^e$	$E_{add}{}^f$
A_HIS	−29.7	—	—	—	—	—
A_HIS′	−27.2	—	—	—	—	—
A_HIS(edge)	−22.5	—	—	—	—	—
3MeA_HIS	−51.7	—	—	—	—	—
3MeA_HIS′	−52.7	—	—	—	—	—
3MeA_HIS(edge)	−61.6	—	—	—	—	—
A_HIS$^+$	−58.4	—	—	—	—	—
A_HIS$^+$(edge)	−66.0	—	—	—	—	—
HIS_A_HIS	−58.7	−59.4	0.7	2.2	−57.2	−1.5
HIS′_A_HIS′	−53.6	−54.4	0.8	2.2	−52.2	−1.4
HIS_A_HIS′	−56.5	−56.9	0.4	1.7	−55.2	−1.3
HIS_A_HIS(edge)	−52.5	−52.2	−0.3	−0.4	−52.6	0.1
HIS′_A_HIS(edge)	−50.8	−49.7	−1.1	0.5	−49.2	−1.6
HIS(edge)_A_HIS(edge)	−41.5	−45.0	3.5	2.6	−42.4	0.9
HIS_A_HIS$^+$	−92.8	−88.1	−4.7	−2.6	−90.7	−2.1
HIS′_A_HIS$^+$	−91.0	−85.6	−5.4	−3.2	−88.8	−2.2
HIS(edge)_A_HIS$^+$	−64.9	−80.9	16.0	11.4	−69.5	4.6
HIS_A_HIS$^+$(edge)	−94.0	−95.7	1.7	3.2	−92.5	−1.5
HIS′_A_HIS$^+$(edge)	−94.5	−93.2	−1.3	1.2	−92.0	−2.5
HIS(edge)_A_HIS$^+$(edge)	−71.4	−88.5	17.1	13.6	−74.9	3.5
HIS_3MeA_HIS	−101.0	−103.5	2.5	2.2	−101.3	0.3
HIS′_3MeA_HIS′	−102.6	−105.3	2.7	2.2	−103.1	0.5
HIS_3MeA_HIS′	−102.2	−104.4	2.2	1.7	−102.7	0.5
HIS_3MeA_HIS(edge)	−109.6	−113.3	3.7	1.9	−111.4	1.8
HIS′_3MeA_HIS(edge)	−110.1	−114.3	4.2	2.2	−112.1	2.0
HIS(edge)_3MeA_HIS(edge)	−115.4	−123.2	7.8	3.9	−119.3	3.9

[a] ΔE is the interaction energy of the dimer or trimer. [b] $\Delta E_{dimer(12)} + \Delta E_{dimer(23)}$ is the sum of the (nearest neighbor) nucleobase−amino acid dimer interaction energies. [c] The synergy energy ($E_{syn} = \Delta E_{trimer(123)} - \Delta E_{dimer(12)} - \Delta E_{dimer(23)}$). [d] $\Delta E_{dimer(13)}$ is the interaction energy of the amino acid-amino acid dimer in the trimer geometry. [e] $\Delta E_{dimer(12)} + \Delta E_{dimer(23)} + \Delta E_{dimer(13)}$ is the sum of all dimer interaction energies. [f] The additivity energy ($E_{add} = \Delta E_{trimer(123)} - \Delta E_{dimer(12)} - \Delta E_{dimer(23)} - \Delta E_{dimer(13)}$).

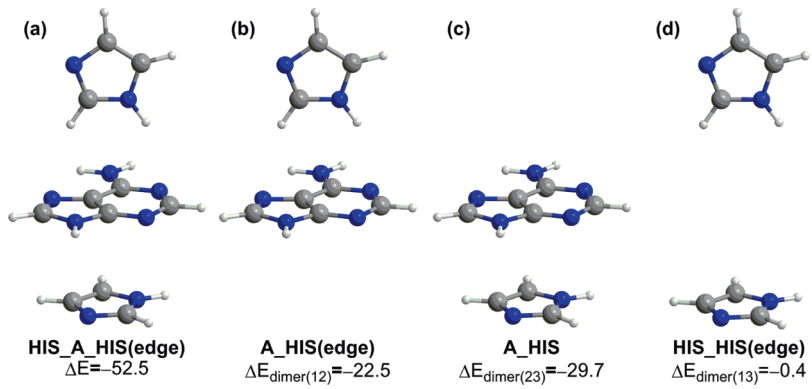

Figure 3. A representative example of the MP2/6-31G*(0.25) interaction energies (kJ mol^{-1}, Table 1) for the HIS_A_HIS(edge) trimer (a), which contains two nearest-neighbor nucleobase−amino acid dimer interactions ((b) T-shaped adenine and histidine (HIS(edge)) and (c) stacked adenine and histidine (HIS)), as well as one histidine−histidine interaction (d).

and $\pi-\pi$ complexes and should not be overlooked in studies of noncovalent interactions.

In most trimers examined in this work, the magnitude of E_{syn} is small, which indicates that the sum of the two nearest-neighbor dimer interactions ($\Delta E_{dimer(12)} + \Delta E_{dimer(23)}$) gives an accurate estimate of the total trimer interaction energy. Specifically, the error is less than 6%. However, there are four trimers (HIS(edge)_A_HIS(edge), HIS(edge)_3MeA_HIS(edge), HIS(edge)_A_HIS$^+$(edge), and HIS(edge)_A_HIS$^+$) that have large E_{syn} values (8, 6, 19, and 20% errors, respectively). In these four systems, there is significant repulsion between the two amino acids (positive $\Delta E_{dimer(13)}$, Table 1). This repulsion arises since two acidic or two basic regions of the amino acids are directed toward one another in the trimers. This suggests that it is important to consider the $\Delta E_{dimer(13)}$ term.

The magnitude of E_{add} is small for all trimers (error is less than 7%), which reveals whether the trimer interactions can be estimated by the sum of the three pairwise interaction energies. Despite smaller additivity than synergy terms, E_{add} values of up to 4.6 kJ mol^{-1} are obtained. It is unknown whether these energies suggest that the trimers are nonadditive or whether they arise from errors in our computational method. For example, deviations could arise due to the large BSSE corrections for these $\pi-\pi$ and $\pi^+-\pi$ complexes at the level of theory implemented. Furthermore, our method for calculating the $\Delta E_{dimer(13)}$ term in the absence of the nucleobase may overestimate the amino acid−amino acid dimer interaction. However, E_{add} is less than 2 kJ mol^{-1} for most trimers. This fact, coupled with the geometric additivity discussed in the previous section, suggests that these interactions are additive. Regardless of the nature of the additivity, our current analysis does not provide information about the individual interactions in the trimers. Specifically, we do not know whether the nucleobase−amino acid interactions are equivalent in dimer and trimer complexes,

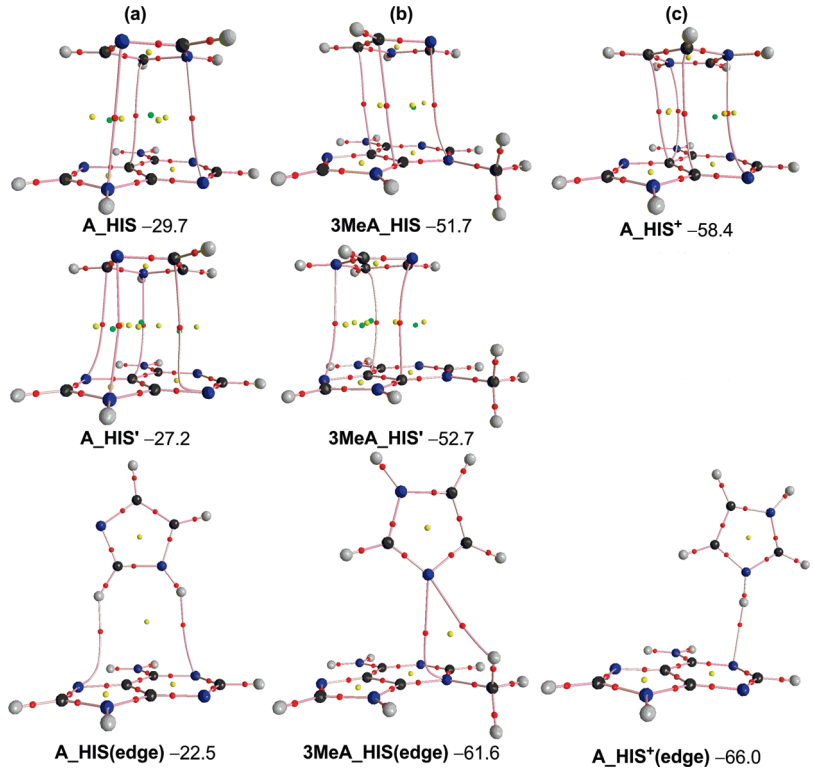

Figure 4. Molecular graphs and MP2/6-31G*(0.25) interaction energies for (a) adenine and histidine stacked (HIS and HIS′) and T-shaped (HIS(edge)) dimers, (b) 3-methyladenine and histidine stacked (HIS and HIS′) and T-shaped (HIS(edge)) dimers, and (c) adenine and protonated histidine stacked (HIS^+) and T-shaped (HIS^+(edge)) dimers. Interaction energies are reported in kJ mol^{-1}.

or whether the nucleobase−amino acid interactions are different in different sized complexes but sum to yield an overall additive interaction. Therefore, in hopes to gain a better understanding of the interplay between nucleobase−amino acid dimers, we will use QTAIM in the following section.

3.3. Quantum Theory of Atoms in Molecules (QTAIM) Analysis. QTAIM can be very useful for analyzing closed-shell bonding interactions.[40−42] Topological analysis of the electron density was initially used to identify the presence of hydrogen-bonding interactions through a bond path connecting a hydrogen atom to a hydrogen acceptor (or electron donor).[46] Furthermore, the maximum electron density on the interatomic surface between these two atoms (i.e., the bond critical point (BCP)) can be correlated to the hydrogen-bond strength,[65] as well as the hydrogen-bond length,[64] while the sum of the electron density at the hydrogen-bond critical points can be correlated with the stability of the complex (see, for example, refs 45 and 55). Therefore, it is not surprising that the vast majority of QTAIM literature on noncovalent interactions has studied hydrogen bonding. However, very few studies have applied QTAIM to stacking and T-shaped interactions.[10,20,26,27,29,32,34−36,44,49,50,52−54,59]

In 2005, Zhikol et al. were the first to analyze stacking interactions with QTAIM.[50] In this study, 10 unique $\pi-\pi$ stacked geometries of the benzene dimer with various degrees of symmetry were characterized. In all these systems, 1 to 12 intermolecular bond paths between the monomers were found. Intriguingly, all dimers were characterized by one, and only one, cage critical point (CCP) between the benzene rings, and it was suggested that the existence of a CCP correlates with the phenomenon of stacking. This work was also the first to suggest that the values of the electron density ($\rho(r)$) and the Laplacian ($\nabla^2\rho(r)$) at the CCP yield a quantitative relationship with the relative dimer binding energies.

Since 2005, a limited number of studies have investigated stacked or T-shaped systems, and each study has had a unique set of objectives. For example, the Mosquera group compared the changes in the electron population of monomers and dimers to quantify charge transfer in the quinhydrone stacked dimer.[54] In addition, the Frontera group examined CCP properties to study the interplay of $\pi-\pi$ stacking[26,34] or $\pi-\pi$ T-shaped[27,29] interactions and other noncovalent (hydrogen bonding, cation−π, anion−π, or small molecule X−H$\cdots\pi$) interactions. The systems investigated by the Frontera group had symmetry constraints, which result in only one CCP. In contrast, multiple CCPs are typically observed for systems with no symmetry.[10,20,44,49,53,54,59] The detailed study by Matta et al.[44] fully characterized the interactions in experimental DNA helices with a focus on identifying BCP properties between stacked base pairs and did not examine the properties of the multiple CCPs in their complexes. Additionally, we are unaware of any studies that have investigated $\pi-\pi$ T-shaped interactions in an asymmetric (C_1) system, even though topological analysis of the electron density may provide an interesting way to confirm the presence of T-shaped interactions through the identification of distinguishing bond paths.

In this work, we first characterize the BCP and CCP properties of nucleobase−amino acid dimers in both $\pi-\pi$ stacked and $\pi-\pi$ T-shaped orientations and relate our findings to previous work in the literature. Subsequently, our 18 trimers will be investigated, where we will discuss how the topology of the electron density in the trimers differs from the corresponding dimers. Our end goal is to gain insight into whether individual nucleobase−amino acid interactions are equivalent or distinct in dimers and trimers.

3.3.1. Dimer Interactions. The molecular graphs for all nucleobase−amino acid dimers considered in this study are shown in Figure 4, while the corresponding BCP properties used to characterize the intermolecular interactions are summarized in Table 2. This table also provides the distances between the two atoms involved in the bonding interaction (bond length,

TABLE 2: Closed-Shell Bonding between Nucleobase−Amino Acid Stacked and T-Shaped Dimers[a]

dimer[b]	bond[c]	BL	BPL	BPL − BL	$\rho(r)$ ($\times 10^3$)	$\nabla^2\rho(r)$ ($\times 10^2$)	λ_1	λ_2	λ_3	ε	$G(r)$	$V(r)$	$H(r)$
A_HIS	N3−N1	3.385	3.408	0.023	6.177	1.865	−0.003	−0.002	0.023	0.677	0.004	−0.004	0.000
	C5−C5	3.321	3.381	0.060	7.258	2.042	−0.003	−0.003	0.026	0.217	0.004	−0.003	0.001
	N9−N3	3.318	3.340	0.022	6.453	1.958	−0.003	−0.002	0.025	0.523	0.004	−0.004	0.000
A_HIS′	N3−C4	3.424	3.938	0.514	6.540	1.916	−0.003	−0.001	0.023	1.576	0.004	−0.003	0.001
	C5−N1	3.367	3.458	0.091	6.282	1.980	−0.003	−0.001	0.024	1.267	0.004	−0.004	0.001
	N9−N3	3.359	3.383	0.024	5.903	1.895	−0.003	−0.001	0.023	2.013	0.004	−0.004	0.000
	N7−C2	3.362	3.403	0.041	6.071	1.938	−0.003	−0.001	0.023	1.392	0.004	−0.003	0.001
A_HIS(edge)	N1−H1	2.739	2.780	0.041	6.207	2.269	−0.005	−0.003	0.031	0.492	0.005	−0.004	0.001
	N7−H2	2.714	2.919	0.205	7.263	2.573	−0.006	−0.002	0.034	1.759	0.005	−0.004	0.001
3MeA_HIS	N3−N3	3.396	3.504	0.108	6.222	1.885	−0.003	−0.001	0.023	1.937	0.004	−0.004	0.000
	C5−C5	3.329	3.368	0.039	6.736	2.184	−0.002	−0.001	0.025	1.146	0.005	−0.004	0.001
	C4−C4	3.393	3.821	0.428	6.252	2.045	−0.002	−0.001	0.023	2.538	0.004	−0.004	0.001
3MeA_HIS′	N7−N1	3.343	3.368	0.025	6.341	1.920	−0.003	−0.002	0.024	0.767	0.004	−0.004	0.000
	C4−N3	3.322	3.362	0.040	6.146	2.200	−0.003	−0.002	0.025	7.789	0.005	−0.004	0.001
	C5−C5	3.384	3.678	0.294	6.848	1.909	−0.002	−0.002	0.023	0.218	0.004	−0.003	0.001
3MeA_HIS(edge)	N3−N3	3.179	3.446	0.267	8.806	2.602	−0.006	−0.002	0.034	2.284	0.006	−0.005	0.000
	H3−N3	2.652	2.704	0.052	8.366	2.858	−0.007	−0.005	0.041	0.468	0.006	−0.005	0.001
A_HIS^+	N3−N1	3.323	3.396	0.073	6.714	2.083	−0.004	−0.001	0.025	18.171	0.005	−0.004	0.000
	C4−C5	3.216	3.284	0.068	7.808	2.560	−0.002	−0.002	0.030	0.144	0.005	−0.004	0.001
	C5−C5′	3.297	3.313	0.016	7.359	2.574	−0.001	−0.001	0.028	0.813	0.005	−0.004	0.001
	C5−N1′	3.294	3.467	0.173	7.195	2.249	−0.004	−0.001	0.027	7.860	0.005	−0.004	0.001
A_HIS^+(edge)	N1−H1	2.126	2.157	0.031	20.709	5.843	−0.022	−0.022	0.103	0.013	0.016	−0.016	0.000

[a] All values (electron density $\rho(r)$, Laplacian of the electron density ($\nabla^2\rho(r)$), the curvatures of the electron density (λ_1, λ_2, and λ_3), the bond ellipticity (ε), the gradient kinetic energy density ($G(r)$), the potential energy density ($V(r)$), and the total electronic energy density ($H(r)$) are reported in atomic units (au), except for bond lengths (BL), bond path lengths (BPL), and their differences (BPL − BL), which are in angstroms (Å). [b] Stacked (HIS, HIS′, or HIS^+) and amino acid edge T-shaped (HIS(edge) or HIS^+(edge)) dimers. [c] Bond critical points are labeled with both atoms involved in bonding, where the first atom belongs to the nucleobase (A or 3MeA) and the second atom belongs to the amino acid (His or His^+). See Figure 1 for atomic numbering.

BL), as well as the corresponding bond path lengths (BPL), where their difference (BPL − BL) can be used to determine the curvature of a bond path. Large BPL−BL differences (up to 0.514 Å) suggest strain in the bonding interactions for some of our complexes. Although some of this strain may be reduced through free optimizations, our results are consistent with previous work, where (for example) highly curved bond paths (BPL − BL ranges from 0.115 to 0.565 Å) were reported for the quinhydrone stacked dimer.[54] The positive values of both the Laplacian ($\nabla^2\rho(r)$) and the total energy density ($H(r)$, Table 2) confirm that all intermolecular bonding considered are of the closed-shell type.

3.3.1.1. Stacked Dimers. QTAIM analysis of the electron density of stacked nucleobase−amino acid dimers reveals three different types of intermolecular bond paths: N−N, C−C, and N−C. The N−N bond paths in nucleobase−amino acid dimers are very similar to those in DNA nucleobase complexes,[44] where the average N−N bond properties are comparable to the present work (in parentheses): BPL = 3.486 (3.400) Å, $\rho(r) = 0.005$ (0.006) au, and $\nabla^2\rho(r) = 0.015$ (0.019) au. Similarly, the uracil-phenylalanine stacked dimer[10] has C−C and C−N bond paths with very similar properties to those observed in the present study (C−C average properties (present work in parentheses): $\rho(r) = 6.949 \times 10^{-3}$ (7.044×10^{-3}) au, and $\nabla^2\rho(r) = 2.048 \times 10^{-2}$ (2.219×10^{-2}) au; C−N average properties (present work in parentheses): $\rho(r) = 7.492 \times 10^{-3}$ (6.447×10^{-3}) au, and $\nabla^2\rho(r) = 2.281 \times 10^{-2}$ (2.057×10^{-2}) au). It should be noted that we do not find any distinguishing differences in the bonding properties for $\pi-\pi$ (A_HIS and A_HIS′) and $\pi^+-\pi$ interactions (3MeA_HIS, 3MeA_HIS′, and A_HIS^+).

It has been suggested by Matta et al.[44] that a bond critical point with $\rho(r)$ of ∼0.006 au can be associated with a bond energy of ∼1 kcal mol^{-1} (or ∼4 kJ mol^{-1}). The authors also suggest that the cumulative effect of several weak bonding interactions leads to non-negligible stabilization energies, where very weak bonding is classified as $\rho(r) < 0.01$ au.[44] In the present work, all BCP electron densities are very similar (∼0.006−0.008 au.) and therefore would be classified as weak bonding interactions. However, when the sum of the electron densities of all intermolecular BCPs is considered, the total BCP electron density is ∼0.019−0.029 au. Using the electron density/bond energy relationship suggested by Matta et al.,[44] a much weaker stabilization than identified through our interaction energy analysis (Table 1) is obtained. This suggests that it may not be possible to describe our systems by simply considering only pairwise contacts between atoms in different monomers.

Although the sum of the electron density at the hydrogen-bond critical point is representative of the stability of a hydrogen-bonded complex,[45,55] and has been previously observed for select stacked systems,[53] we do not see a similar trend for our stacked systems. This discrepancy may arise since our dimers have different numbers of intermolecular bond paths. It is intriguing that the average BCP electron density predicts that A_HIS′ (average $\rho(r) = 6.199 \times 10^{-3}$ au) < A_HIS (average $\rho(r) = 6.629 \times 10^{-3}$ au), and 3MeA_HIS (average $\rho(r) = 6.403 \times 10^{-3}$ au) < 3MeA_HIS′ (average $\rho(r) = 6.445 \times 10^{-3}$ au), which corresponds to the binding energy trends. Nevertheless, this correlation could be a coincidence since the trend in binding energies for all stacked dimers cannot be predicted from the average BCP electron densities.[53]

As previously mentioned, it has been proposed that cage critical points can be used to identify stacking interactions.[50] Indeed, we identify one to three CCPs in our C_1 symmetric stacked dimers, where the corresponding $\rho(r)$ and $\nabla^2\rho(r)$ are reported in Table 3. Although discussion of multiple CCPs is limited in the literature,[20,49,54,59] close examination of published molecular graphs reveals more than one cage critical point in stacked systems of low symmetry.[10,20,44,49,53,54,59] Since more than one CCP is present on our complexes, it is difficult to relate complex stability to the cage critical point properties as previously proposed in the literature.[50] However, the average CCP properties predict that A_HIS′ (average $\rho(r) = 4.616 \times 10^{-3}$

TABLE 3: Charge Density ($\rho(r)$, au) and Laplacian ($\nabla^2\rho(r)$, au) at the Cage Critical Points for Nucleobase−Amino Acid Dimers[a]

dimer[b]	CCP position[c]	$\rho(r)$ ($\times 10^3$)	$\nabla^2\rho(r)$ ($\times 10^2$)
A_HIS	C4−C5	4.257	2.067
	N7	5.034	2.025
A_HIS′	C2	4.411	1.773
	C4−C5	4.748	1.951
	N7	4.688	1.980
3MeA_HIS	C2	3.937	1.722
3MeA_HIS′	C2	4.355	1.680
	C4−C5	4.588	2.024
	N7	4.581	2.006
A_HIS$^+$	C2	4.704	2.071

[a] All values are reported in atomic units (au). [b] Stacked (HIS, HIS′, or HIS$^+$) and amino acid edge T-shaped (HIS(edge) or HIS$^+$(edge)) dimer orientations. [c] Cage critical points lie in a plane between the nucleobase and amino acid and are labeled relative to the nucleobase atoms. See Figure 1 for atomic numbering and Figure 3 for molecular graphs.

au) < A_HIS (average $\rho(r) = 6.646 \times 10^{-3}$ au), and 3MeA_HIS (average $\rho(r) = 3.937 \times 10^{-3}$ au) < 3MeA_HIS′ (average $\rho(r) = 4.508 \times 10^{-3}$ au), which again matches the trend in Table 1. Nevertheless, the trend in the binding energies across all stacked dimers cannot be predicted. Therefore, our results indicate that CCP properties have a weak correlation with binding strength for C_1 symmetric systems, which is consistent with results for the uracil−phenylalanine dimer.[10]

3.3.1.2. T-shaped Dimers. QTAIM analysis of $\pi-\pi$ and $\pi^+-\pi$ T-shaped interactions reveals two types of intermolecular nucleobase−amino acid bond paths: N−N and N−H. The N−N bond path is only observed in the 3MeA_HIS(edge) dimer (Table 2 and Figure 4, bottom), where the basic N atom of histidine prefers to be in close contact with the (formally) positively charged N atom in 3-methyladenine. This dimer also has an N−H bond path connecting the basic N3 atom in histidine with the acidic H on the C3 methyl group in 3-methyladenine. In the other dimers, N−H bond paths are observed between acidic hydrogens in the monomer edge and the basic N atoms in adenine. The greater similarity is found for these bond paths and those for hydrogen-bonding compared to those for stacking interactions, confirming the larger electrostatic nature of these $\pi-\pi$ T-shaped interactions.

Closer examination of the electron density at the N−H bond critical points (Table 2) indicates that these bond paths are weak (∼0.006−0.008 au for A_HIS(edge) and 3MeA_HIS(edge)). In fact, these BCP electron densities are very similar to those observed for our nucleobase−amino acid stacking interactions. Indeed, even the very strong A_HIS$^+$(edge) interaction (−66.0 kJ mol^{-1}), which has one N−H bond path with a BCP electron density of 0.021 au, has a weaker bond path compared to the cytosine and guanine Watson−Crick hydrogen-bonded dimer (average N−H BCP $\rho(r)$ of 0.038 au).[44] These results collectively confirm that $\pi-\pi$ T-shaped interactions have properties distinct from hydrogen-bonding interactions.

Even though our T-shaped systems have different numbers of intermolecular bond paths, we can predict their trend in stability by considering the sum of the electron density at the intermolecular bond critical points. Interestingly, the binding energy trends are also predicted from the average BCP electron densities. However, it is difficult to know if these trends will hold when a greater number of T-shaped interactions are examined. Additionally, if we attempt to compare T-shaped and stacked dimers, a clear trend in the relative stabilities can no longer be predicted.

No cage critical points are found in our T-shaped dimers. This is not consistent with previous work by the Frontera group that reported one CCP for (C_{2v} or C_s) symmetric $\pi-\pi$ T-shaped systems.[27,29] Due to the symmetry constraints imposed in the complexes studied by Frontera et al., it is not surprising that these systems have one cage critical point (CCP), which the authors then use to characterize the noncovalent interactions present in the system. However, our results indicate that low symmetry T-shaped dimers do not necessarily have cage critical points. Therefore, further investigations must be done to understand the topology of the electron density in the same $\pi-\pi$ T-shaped dimers with and without symmetry constraints.

Although previous literature used the electron density distribution to examine the relative stability of stacked and T-shaped complexes,[10,20,32,44,49,50,52−54] no clear trends are observed for our nucleobase−amino acid dimers. For example, neither the total electron density at intermolecular BCPs nor CCPs can accurately predict relative stacking strengths. Although some promise is seen when the average electron density at BCP or CCP is considered, trends across stacked dimers containing different monomers are not correct. Since various $\pi-\pi$ and $\pi^+-\pi$ interactions may involve too many relative differences in the electron density to definitively provide stability trends, we propose that more work must be done to conclusively determine how systematic changes in the geometry and size of the complex alter QTAIM predictions of complex stability. Even though our results show there is potential for predicting the relative strength of T-shaped interactions, our low-symmetry T-shaped dimers have no CCPs, which contrasts previous literature.[27,29] Therefore, more work needs to be done to bridge the current gap in QTAIM analysis of T-shaped interactions, where future studies should concentrate on how symmetry alters conclusions based on the electron density.

3.3.2. Trimer Interactions. Since QTAIM properties have been used by many authors to examine the interplay between two noncovalent interactions in trimer complexes,[10,20,26−34,39] our 18 trimers were investigated, where Tables 4−6 summarize the values of the electron density ($\rho(r)$) and the Laplacian of the electron density ($\nabla^2\rho(r)$) computed at the bond critical points (stacked and T-shaped) and cage critical points (stacked only) between the nucleobase and amino acid monomers in amino acid−nucleobase−amino acid trimers. These tables also show the differences between the BCP and CCP properties for the trimer and the corresponding dimer ($\Delta\rho(r)$ and $\Delta(\nabla^2\rho(r))$).

In agreement with the geometric additivity discussed in section 3.1, the molecular graphs for most trimers (Figure SI-1−SI-3, Supporting Information) are superpositions of those for the corresponding dimers (compare, for example, Figures 4 and 5). However, for six trimers, extensive searching within AIM2000,[73] as well as AIMAll,[72] was unable to identify critical points that were present in the dimers. For the HIS′_A_HIS′, HIS_A_HIS′, HIS′_A_HIS$^+$, HIS′_A_HIS(edge), and HIS′_A_HIS$^+$(edge) trimers, we were unable to characterize the bond path connecting N7 of adenine and C2 of histidine in the HIS′_A interaction. Also, in the HIS_A_HIS$^+$ and HIS′_A_HIS$^+$ trimer, we were unable to locate the bond path connecting N3 of adenine and N1 of protonated histidine in the A_HIS$^+$ interaction. In HIS′_A_HIS$^+$, the CCP near N7 for the HIS′_A interaction was also not characterized. Although the Poincaré−Hopf relationship[40−42] is satisfied for all trimers, this condition does not verify that critical points were not missed.[40−42] Therefore, it is not clear whether missing critical points indicate changes in the electron densities between monomers in dimers

TABLE 4: Charge Density (ρ_b, au) and Laplacian ($\nabla^2\rho_b$, au) at the Bond and Cage Critical Points for His:A:His Trimers, and Their Variation ($\Delta\rho_b$ and $\Delta(\nabla^2\rho_b)$) with Respect to the Dimers

trimer	dimer[a]	BCP or CCP[b]		$\rho(r)$ ($\times10^3$)	$\nabla^2\rho(r)$ ($\times10^2$)	$\Delta\rho(r)$ ($\times10^3$)	$\Delta(\nabla^2\rho(r))$ ($\times10^2$)
HIS_A_HIS	A_HIS	BCP	N3−N1	6.165	1.826	−0.012	−0.039
		BCP	C5−C5	7.274	2.057	0.016	0.015
		BCP	N9−N3	6.391	1.918	−0.062	−0.040
		CCP	C4−C5	4.358	2.075	0.101	0.008
		CCP	N7	5.054	2.003	0.020	−0.022
HIS′_A_HIS′	A_HIS′	BCP	N3−C4	6.803	1.857	0.263	−0.059
		BCP	C5−N1	6.450	2.041	0.168	0.061
		BCP	N9−N3	6.247	1.896	0.344	0.001
		CCP	C2	4.382	1.768	−0.029	−0.005
		CCP	C4−C5	4.602	1.912	−0.146	−0.039
		CCP	N7	4.702	1.917	0.014	−0.063
HIS_A_HIS′	A_HIS	BCP	N3−N1	6.186	1.828	0.009	−0.037
		BCP	C5−C5	7.276	2.056	0.018	0.014
		BCP	N9−N3	6.390	1.918	−0.063	−0.040
		CCP	C4−C5	4.357	2.077	0.100	0.010
		CCP	N7	5.054	2.000	0.020	−0.025
	A_HIS′	BCP	N3−C4	6.788	1.856	0.248	−0.060
		BCP	C5−N1	6.496	2.043	0.214	0.063
		BCP	N9−N3	6.246	1.897	0.343	0.002
		CCP	C2	4.372	1.765	−0.039	−0.008
		CCP	C4−C5	4.604	1.912	−0.144	−0.039
		CCP	N7	4.704	1.919	0.016	−0.061
HIS_A_HIS(edge)	A_HIS	BCP	N3−N1	6.132	1.828	−0.045	−0.037
		BCP	C5−C5	7.268	2.054	0.010	0.012
		BCP	N9−N3	6.317	1.918	−0.136	−0.040
		CCP	C4−C5	4.317	2.079	0.060	0.012
		CCP	N7	5.043	2.000	0.009	−0.025
	A_HIS(edge)	BCP	N1−H1	5.889	2.201	−0.318	−0.068
		BCP	N7−H2	7.767	2.690	0.504	0.117
HIS′_A_HIS(edge)	A_HIS′	BCP	N3−C4	6.758	1.858	0.218	−0.058
		BCP	C5−N1	6.462	2.043	0.180	0.063
		BCP	N9−N3	6.172	1.898	0.269	0.003
		CCP	C2	4.355	1.767	−0.056	−0.006
		CCP	C4−C5	4.590	1.912	−0.158	−0.039
		CCP	N7	4.691	1.907	0.003	−0.073
	A_HIS(edge)	BCP	N1−H1	5.927	2.203	−0.280	−0.066
		BCP	N7−H2	7.736	2.691	0.473	0.118
HIS(edge)_A_HIS(edge)	A_HIS(edge)	BCP	N1−H1	5.844	2.192	−0.363	−0.077
		BCP	N7−H2	7.691	2.688	0.428	0.115

[a] Stacked (HIS, HIS′) and amino acid edge T-shaped (HIS(edge)) dimers within the trimers. [b] Bond critical points are labeled with both atoms involved in bonding, where the first atom belongs to the nucleobase (A) and the second atom belongs to the amino acid (His). Cage critical points lie in a plane between the nucleobase and amino acid and are labeled relative to the nucleobase atoms. See Figure 1 for atomic numbering.

and trimers, or whether we were simply unsuccessful in finding critical points on very disperse electron density surfaces.

Examination of Tables 4−6 reveals inconsistencies in our QTAIM analysis and our interaction energy decomposition (Table 1). For example, in the HIS(edge)_A_HIS(edge) trimer (Figure 5a), E_{syn} and E_{add} suggest that the T-shaped interactions in the trimer are weaker than in the corresponding dimer. However, the BCP properties indicate that the electron density in the N1−H1 bond path is weaker and the N7−H2 bond path is stronger in the trimer, and the overall changes in the electron density (0.000 13 au) suggest this trimer should exhibit stronger binding than predicted from the sum of the dimer interactions. Additionally, our calculated binding strengths suggest that the HIS_3MeA_HIS′ trimer (Figure 5b) is weaker than predicted by the dimer interaction energies (Table 1), while the overall magnitudes of the electron densities and Laplacian differences (Table 5) suggest a stronger trimer. However, both the BCP and CCP properties indicate that the 3MeA_HIS′ interaction is stronger in this trimer. BCP properties for 3MeA_HIS indicate a stronger stacking interaction in the trimer, while the CCP properties indicate a weaker stacking interaction. Similarly, the HIS(edge)_A_HIS$^+$ trimer (Figure 5c) has a less than additive interaction energy (Table 1), but the overall magnitudes of the electron densities and Laplacian differences suggest a stronger trimer. Furthermore, QTAIM suggests that the HIS(edge)_A T-shaped interaction is weaker in the trimer, but the BCP properties suggest a weaker A_HIS$^+$ stacking interaction in the trimer, while the CCP properties suggest a stronger interaction. Therefore, depending on the trimer considered, our QTAIM results may or may not be in agreement with our previous interaction energy decomposition and it is still unclear whether BCP or CCP properties of the dimers and trimers should be compared.

For all trimers investigated, the magnitude of the difference between the dimer and trimer BCP and CCP properties is extremely small. It is still not clear if these differences are too small to be conclusive within the errors of the computational methods implemented,[32,59] or if real changes in stacked and T-shaped systems are simply too subtle to detect with certainty. Indeed, there is not a clear consensus in the literature if QTAIM results like those presented in this paper are indicative of additive interactions.[20,26,30,32] This is partially a result of few investigations on $\pi-\pi$ and $\pi^+-\pi$ stacking and T-shaped interactions.[10,20,26,27,29,32,34−36,44,49,50,52−54,59] There-

TABLE 5: Charge Density (ρ_b, au) and Laplacian ($\nabla^2\rho_b$, au) at the Bond and Cage Critical Points for His:3MeA:His Trimers, and Their Variation ($\Delta\rho_b$ and $\Delta(\nabla^2\rho_b)$) with Respect to the Dimers

trimer	dimer[a]	BCP or CCP[b]		$\rho(r)$ ($\times10^3$)	$\nabla^2\rho(r)$ ($\times10^2$)	$\Delta\rho(r)$ ($\times10^3$)	$\Delta(\nabla^2\rho(r))$ ($\times10^2$)
HIS_3MeA_HIS	3MeA_HIS	BCP	N3−N3	6.344	1.912	0.122	0.027
		BCP	C5−C5	6.854	2.189	0.118	0.005
		BCP	C4−C4	6.459	2.139	0.207	0.094
		CCP	C2	3.811	1.717	−0.126	−0.005
HIS′_3MeA_HIS′	3MeA_HIS′	BCP	N7−N1	6.378	1.918	0.037	−0.002
		BCP	C4−N3	6.196	2.186	0.050	−0.014
		BCP	C5−C5	6.869	1.904	0.021	−0.005
		CCP	C2	6.834	1.666	2.479	−0.014
		CCP	C4−C5	4.611	2.025	0.023	0.001
		CCP	N7	4.618	2.004	0.037	−0.002
HIS_3MeA_HIS′	3MeA_HIS	BCP	N3−N3	6.349	1.909	0.127	0.024
		BCP	C5−C5	6.844	2.195	0.108	0.011
		BCP	C4−C4	6.454	2.140	0.202	0.095
		CCP	C2	3.827	1.716	−0.110	−0.006
	3MeA_HIS′	BCP	N7−N1	6.406	1.916	0.065	−0.004
		BCP	C4−N3	6.206	2.184	0.060	−0.016
		BCP	C5−C5	6.871	1.902	0.023	−0.007
		CCP	C2	4.392	1.670	0.037	−0.010
		CCP	C4−C5	4.619	2.029	0.031	0.005
		CCP	N7	4.655	2.006	0.074	0.000
HIS_3MeA_HIS(edge)	3MeA_HIS	BCP	N3−N3	6.340	1.907	0.118	0.022
		BCP	C5−C5	6.821	2.208	0.085	0.024
		BCP	C4−C4	6.462	2.144	0.210	0.099
		CCP	C2	3.817	1.720	−0.120	−0.002
	3MeA_HIS(edge)	BCP	N3−N3	9.756	2.836	0.950	0.234
		BCP	H3−N3	8.219	2.794	−0.147	−0.064
HIS′_3MeA_HIS(edge)	3MeA_HIS′	BCP	N7−N1	6.340	1.923	−0.001	0.003
		BCP	C4−N3	6.203	2.194	0.057	−0.006
		BCP	C5−C5	6.866	1.911	0.018	0.002
		CCP	C2	4.391	1.675	0.036	−0.005
		CCP	C4−C5	4.608	2.025	0.020	0.001
		CCP	N7	4.600	2.005	0.019	−0.001
	3MeA_HIS(edge)	BCP	N3−N3	9.827	2.861	1.021	0.259
		BCP	H3−N3	8.297	2.821	−0.069	−0.037
HIS(edge)_3MeA_HIS(edge)	3MeA_HIS(edge)	BCP	N3−N3	9.857	2.853	1.051	0.251
		BCP	H3−N3	8.296	2.823	−0.070	−0.035

[a] Stacked (HIS, HIS′) and amino acid edge T-shaped (HIS(edge)) dimers within the trimers. [b] Bond critical points are labeled with both atoms involved in bonding, where the first atom belongs to the nucleobase (3MeA) and the second atom belongs to the amino acid (His). Cage critical points lie in a plane between the nucleobase and amino acid and are labeled relative to the nucleobase atoms. See Figure 1 for atomic numbering.

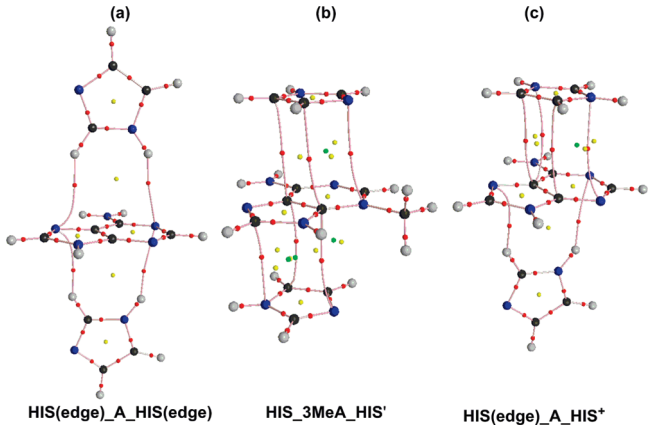

Figure 5. Molecular graphs for the (a) HIS(edge)_A_HIS(edge) trimer where one histidine is T-shaped (HIS(edge)) and the other histidine is T-shaped (HIS(edge)) relative to adenine, (b) HIS_3MeA_HIS′ trimer where one histidine is stacked (HIS) and the other histidine is flipped prior to stacking with 3-methyladenine (HIS′), and (c) HIS(edge)_A_HIS$^+$ trimer where histidine is T-shaped (HIS(edge)) and protonated histidine is stacked (HIS$^+$) relative to adenine.

fore, we propose that more studies are required to clarify how QTAIM can improve our understanding of whether these interactions change in dimer and trimer systems.

It is clear from the literature that QTAIM can provide powerful information about hydrogen-bonding interactions, which is likely due to the large electron density shared between two monomers with very specific atomic contacts. However, since the small electron densities are delocalized over the entire π-system in stacked and T-shaped complexes, several pairwise contacts are described by a QTAIM analysis. In reality, these $\pi-\pi$ systems are difficult to describe with specific atomic contacts between the two monomers, and care should be taken when applying QTAIM analysis for these types of interactions.[59] Therefore, we suggest that additional studies should develop new methods that are sensitive to disperse electron densities, and able to identify and quantify $\pi-\pi$ and $\pi^+-\pi$ stacking and T-shaped interaction changes in dimers and trimers.

4. Conclusions

Due to the potential importance of the interplay between noncovalent interactions in nature, this paper investigated the geometric and energetic additivity in amino acid−nucleobase−amino acid trimers containing adenine or its (cationic) damaged counterpart, 3-methyladenine, and histidine, in both the neutral and protonated forms. For six test trimers, extensive scans of the PES reveal that both stacked and T-shaped interactions, as well as both $\pi-\pi$ and $\pi^+-\pi$ interactions, exhibit geometric

TABLE 6: Charge Density (ρ_b, au) and Laplacian ($\nabla^2\rho_b$, au) at the Bond and Cage Critical Points for His:A:His$^+$ Trimers, and Their Variation ($\Delta\rho_b$ and $\Delta(\nabla^2\rho_b)$) with Respect to the Dimers

trimer	dimer[a]	BCP or CCP[b]		$\rho(r)$ ($\times10^3$)	$\nabla^2\rho(r)$ ($\times10^2$)	$\Delta\rho(r)$ ($\times10^3$)	$\Delta(\nabla^2\rho(r))$ ($\times10^2$)
HIS_A_HIS$^+$	A_HIS	BCP	N3−N1	6.117	1.830	−0.060	−0.035
		BCP	C5−C5	7.308	2.040	0.050	−0.002
		BCP	N9−N3	6.263	1.902	−0.190	−0.056
		CCP	C4−C5	4.300	2.077	0.043	0.010
		CCP	N7	5.085	1.948	0.051	−0.077
	A_HIS$^+$	BCP	C4−C5	7.854	2.560	0.046	0.000
		BCP	C5−C5′	7.412	2.544	0.053	−0.030
		BCP	C5−N1′	7.216	2.241	0.021	−0.008
		CCP	C2	4.751	2.059	0.047	−0.012
HIS′_A_HIS$^+$	A_HIS′	BCP	N3−C4	6.778	1.851	0.238	−0.065
		BCP	C5−N1	6.441	2.040	0.159	0.060
		BCP	N9−N3	6.164	1.883	0.261	−0.012
		CCP	C2	4.365	1.749	−0.046	−0.024
		CCP	C4−C5	4.541	1.907	−0.207	−0.044
	A_HIS$^+$	BCP	C4−C5	7.850	2.561	0.042	0.001
		BCP	C5−C5′	7.389	2.553	0.030	−0.021
		BCP	C5−N1′	7.220	2.240	0.025	−0.009
		CCP	C2	4.767	2.061	0.063	−0.010
HIS(edge)_A_HIS$^+$	A_HIS(edge)	BCP	N1−H1	5.779	2.184	−0.428	−0.085
		BCP	N7−H2	7.642	2.680	0.379	0.107
	A_HIS$^+$	BCP	N3−N1	6.696	2.082	−0.018	−0.001
		BCP	C4−C5	7.802	2.558	−0.006	−0.002
		BCP	C5−C5′	7.365	2.552	0.006	−0.022
		BCP	C5−N1′	7.161	2.246	−0.034	−0.003
		CCP	C2	4.717	2.061	0.013	−0.010
HIS_A_HIS$^+$(edge)	A_HIS	BCP	N3−N1	6.175	1.840	−0.002	−0.025
		BCP	C5−C5	7.332	2.029	0.074	−0.013
		BCP	N9−N3	6.226	1.896	−0.227	−0.062
		CCP	C4−C5	4.279	2.085	0.022	0.018
		CCP	N7	4.986	1.907	−0.048	−0.118
	A_HIS$^+$(edge)	BCP	N1−H1	19.707	5.585	−1.002	−0.258
HIS′_A_HIS$^+$(edge)	A_HIS′	BCP	N3−C4	6.777	1.852	0.237	−0.064
		BCP	C5−N1	6.491	2.036	0.209	0.056
		BCP	N9−N3	6.176	1.892	0.273	−0.003
		CCP	C2	4.343	1.759	−0.068	−0.014
		CCP	C4−C5	4.560	1.923	−0.188	−0.028
		CCP	N7	4.667	1.891	−0.021	−0.089
	A_HIS$^+$(edge)	BCP	N1−H1	20.507	5.760	−0.202	−0.083
HIS(edge)_A_HIS$^+$(edge)	A_HIS(edge)	BCP	N1−H1	5.538	2.118	−0.669	−0.151
		BCP	N7−H2	7.822	2.784	0.559	0.211
	A_HIS$^+$(edge)	BCP	N1−H1	20.665	5.915	−0.044	0.072

[a] Stacked (HIS, HIS′, HIS$^+$) and amino acid edge T-shaped (HIS(edge) or HIS$^+$(edge)) dimers within the trimers. [b] Bond critical points are labeled with both atoms involved in bonding, where the first atom belongs to the nucleobase (A) and the second atom belongs to the amino acid (His or His$^+$). Cage critical points lie in a plane between the nucleobase and amino acid and are labeled relative to the nucleobase atoms. See Figure 1 for atomic numbering.

additivity. Subsequently, to determine the energetic additivity, we examined the synergy (E_{syn}) and the additivity (E_{add}) energy. E_{syn} reveals that the sum of the two nucleobase−amino acid interactions is a fairly good estimate of the total trimer interaction energy. However, an even better estimate of the trimer interaction energy is obtained when the interaction between the two amino acids ($\Delta E_{dimer(13)}$) is also taken into account (E_{add}). Additionally, E_{syn} and E_{add} indicate that $\pi^+-\pi$ interactions are quite different from $\pi-\pi$ interactions, as well as the cation$-\pi$ interactions (involving a cationic point charge) typically examined in trimers. Therefore, our results reemphasize the previous work of Singh et al.,[25] which proposed that $\pi^+-\pi$ interactions are a unique type of noncovalent interaction.

The generally small magnitude of E_{add} (< 2 kJ mol^{-1}) suggests that these interactions are additive. Nevertheless, our interaction energy analysis does not reveal whether the nucleobase−amino acid interactions are equivalent in dimers and trimers, or whether the nucleobase−amino acid interactions differ in different sized complexes but sum to yield an overall additive interaction. Although QTAIM has shown promise for investigating the interplay of various interactions in trimers,[10,20,26−34,39] conclusions from our QTAIM analysis and our interaction energy evaluation are inconsistent. Furthermore, the magnitudes of the differences between the dimer and trimer BCP and CCP properties are extremely small and cannot be expected to give concrete descriptions of the changes (if any) between the dimers and trimers.[32,59] Due to the limited number of stacking and T-shaped QTAIM investigations in the literature, we propose that more studies are required to clarify how QTAIM can improve our understanding of the differences between $\pi-\pi$ and $\pi^+-\pi$ interactions in dimers and trimers. Furthermore, close examination of the literature indicates that there is no consensus on which QTAIM properties best describe these disperse interactions and should be analyzed to identify and predict the stability of $\pi-\pi$ stacked and T-shaped interactions.[10,20,32,44,49,50,52−54] Therefore, we propose that more work needs to be done to determine how the geometry, symmetry, and system size alter the QTAIM properties. Finally, the small intermolecular electron densities in stacked and T-shaped systems are delocalized over the entire π-system, which makes it difficult to describe these interactions

through specific atomic contacts between two monomers. Therefore, we suggest that additional studies must strive to develop new methods that are sensitive enough to identify and quantify differences in $\pi-\pi$ and $\pi^{+}-\pi$ stacking and T-shaped interactions in dimer and trimer systems.

Acknowledgment. We thank the Canada Foundation for Innovation (CFI), the Natural Sciences and Engineering Research Council (NSERC), and the Canada Research Chair program for financial support. We acknowledge the Upscale and Robust Abacus for Chemistry In Lethbridge (URACIL) for computer resources. L.R.R. thanks NSERC (CGS-D) and Alberta Ingenuity Fund (AIF) for student scholarships. C.D.M.C. also thanks NSERC for an undergraduate student research award (USRA).

Supporting Information Available: Full potential energy surface scans for the HIS_A_HIS(edge) and HIS′_3MeA_HIS′ trimers, geometric variables (R_1, α, and R_2 values) used to construct all trimers in this study, and molecular graphs of all 18 trimers. This material is available free of charge via the Internet at http://pubs.acs.org.

References and Notes

(1) Stivers, J. T.; Jiang, Y. L. *Chem. Rev.* **2003**, *103*, 2729–2759.
(2) Berti, P. J.; McCann, J. A. B. *Chem. Rev.* **2006**, *106*, 506–555.
(3) Dalhus, B.; Laerdahl, J. K.; Backe, P. H.; Bjoras, M. *FEMS Microbiol. Rev.* **2009**, *33*, 1044–1078.
(4) Hoglund, A.; Kohlbacher, O. *Proteome Sci.* **2004**, *2*, 3.
(5) Luscombe, N. M.; Laskowski, R. A.; Thornton, J. M. *Nucleic Acids Res.* **2001**, *29*, 2860–2874.
(6) Mao, L.; Wang, Y.; Liu, Y.; Hu, X. *J. Mol. Biol.* **2004**, *336*, 787–807.
(7) Copeland, K. L.; Anderson, J. A.; Farley, A. R.; Cox, J. R.; Tschumper, G. S. *J. Phys. Chem. B* **2008**, *112*, 14291–14295.
(8) Cauet, E.; Rooman, M.; Wintjens, R.; Lievin, J.; Biot, C. *J. Chem. Theory Comput.* **2005**, *1*, 472–483.
(9) Cysewski, P. *Phys. Chem. Chem. Phys.* **2008**, *10*, 2636–2645.
(10) Ebrahimi, A.; Habibi-Khorassani, M.; Gholipour, A. R.; Masoodi, H. R. *Theor. Chem. Acc.* **2009**, *124*, 115–122.
(11) Rutledge, L. R.; Campbell-Verduyn, L. S.; Wetmore, S. D. *Chem. Phys. Lett.* **2007**, *444*, 167–175.
(12) Rutledge, L. R.; Durst, H. F.; Wetmore, S. D. *Phys. Chem. Chem. Phys.* **2008**, *10*, 2801–2812.
(13) Rutledge, L. R.; Durst, H. F.; Wetmore, S. D. *J. Chem. Theory Comput.* **2009**, *5*, 1400–1410.
(14) Churchill, C. D. M.; Wetmore, S. D. *J. Phys. Chem. B* **2009**, *113*, 16046–16058.
(15) Rutledge, L. R.; Wetmore, S. D. *J. Chem. Theory Comput.* **2008**, *4*, 1768–1780.
(16) Wyatt, M. D.; Allan, J. M.; Lau, A. Y.; Ellenberger, T. E.; Samson, L. D. *Bioessays* **1999**, *21*, 668–676.
(17) Lau, A. Y.; Wyatt, M. D.; Glassner, B. J.; Samson, L. D.; Ellenberger, T. *Proc. Natl. Acad. Sci. U.S.A.* **2000**, *97*, 13573–13578.
(18) Tauer, T. P.; Sherrill, C. D. *J. Phys. Chem. A* **2005**, *109*, 10475–10478.
(19) Sinnokrot, M. O.; Sherrill, C. D. *J. Phys. Chem. A* **2006**, *110*, 10656–10668.
(20) Ebrahimi, A.; Habibi, M.; Neyband, R. S.; Gholipour, A. R. *Phys. Chem. Chem. Phys.* **2009**, *11*, 11424–11431.
(21) Sponer, J.; Gabb, H. A.; Leszczynski, J.; Hobza, P. *Biophys. J.* **1997**, *73*, 76–87.
(22) Kabelac, M.; Sherer, E. C.; Cramer, C. J.; Hobza, P. *Chem.—Eur. J.* **2007**, *13*, 2067–2077.
(23) Kabelac, M.; Valdes, H.; Sherer, E. C.; Cramer, C. J.; Hobza, P. *Phys. Chem. Chem. Phys.* **2007**, *9*, 5000–5008.
(24) Vijay, D.; Zipse, H.; Sastry, G. N. *J. Phys. Chem. B* **2008**, *112*, 8863–8867.
(25) Singh, N. J.; Min, S. K.; Kim, D. Y.; Kim, K. S. *J. Chem. Theory Comput.* **2009**, *5*, 515–529.
(26) Quinonero, D.; Frontera, A.; Escudero, D.; Ballester, P.; Costa, A.; Deya, P. M. *Theor. Chem. Acc.* **2008**, *120*, 385–393.
(27) Escudero, D.; Frontera, A.; Quinonero, D.; Deya, P. M. *J. Phys. Chem. A* **2008**, *112*, 6017–6022.
(28) Escudero, D.; Frontera, A.; Quinonero, D.; Deya, P. M. *Chem. Phys. Lett.* **2008**, *456*, 257–261.
(29) Escudero, D.; Estarellas, C.; Frontera, A.; Quinonero, D.; Deya, P. M. *Chem. Phys. Lett.* **2009**, *468*, 280–285.
(30) Estarellas, C.; Frontera, A.; Quinonero, D.; Alkorta, I.; Deya, P. M.; Elguero, J. *J. Phys. Chem. A* **2009**, *113*, 3266–3273.
(31) Estarellas, C.; Frontera, A.; Quinonero, D.; Deya, P. M. *Chem. Phys. Lett.* **2009**, *479*, 316–320.
(32) Estevez, L.; Otero, N.; Mosquera, R. A. *J. Phys. Chem. A* **2009**, *113*, 11051–11058.
(33) Grabowski, S. J.; Leszczynski, *J. Chem. Phys.* **2009**, *355*, 169–176.
(34) Quinonero, D.; Frontera, A.; Garau, C.; Ballester, P.; Costa, A.; Deya, P. M. *Chemphyschem* **2006**, *7*, 2487–2491.
(35) Estarellas, C.; Escudero, D.; Frontera, A.; Quinonero, D.; Deya, P. M. *Theor. Chem. Acc.* **2009**, *122*, 325–332.
(36) Frontera, A.; Quinonero, D.; Costa, A.; Ballester, P.; Deya, P. M. *New J. Chem.* **2007**, *31*, 556–560.
(37) Antony, J.; Bruske, B.; Grimme, S. *Phys. Chem. Chem. Phys.* **2009**, *11*, 8440–8447.
(38) Pakiari, A. H.; Fakhraee, S. *J. Theor. Comput. Chem.* **2006**, *5*, 621–631.
(39) Ziolkowski, M.; Grabowski, S. J.; Leszczynski, J. *J. Phys. Chem. A* **2006**, *110*, 6514–6521.
(40) Bader, R. F. W. *Atoms in Molecules: A Quantum Theory; International Series of Monographs on Chemistry*; Clarendon Press: New York, 1990; Vol. 22.
(41) Popelier, P. L. A. *Atoms in Molecules: An Introduction*; Prentice Hall: London, 2000.
(42) Matta, C. F.; Boyd, R. J., Eds. *The Quantum Theory of Atoms in Molecules: From Solid State to DNA and Drug Design*; Wiley-VCH: Weinheim, Germany, 2007.
(43) Bader, R. F. W. *J. Phys. Chem. A* **2009**, *113*, 10391–10396.
(44) Matta, C. F.; Castillo, N.; Boyd, R. J. *J. Phys. Chem. B* **2006**, *110*, 563–578.
(45) LaPointe, S. M.; Farrag, S.; Bohorquez, H. J.; Boyd, R. J. *J. Phys. Chem. B* **2009**, *113*, 10957–10964.
(46) Koch, U.; Popelier, P. L. A. *J. Phys. Chem.* **1995**, *99*, 9747–9754.
(47) Hobza, P.; Sponer, J.; Cubero, E.; Orozco, M.; Luque, F. J. *J. Phys. Chem. B* **2000**, *104*, 6286–6292.
(48) Parthasarathi, R.; Amutha, R.; Subramanian, V.; Nair, B. U.; Ramasami, T. *J. Phys. Chem. A* **2004**, *108*, 3817–3828.
(49) Parthasarathi, R.; Subramanian, V. *Structural Chem.* **2005**, *16*, 243–255.
(50) Zhikol, O. A.; Shishkin, O. V.; Lyssenko, K. A.; Leszczynski, J. *J. Chem. Phys.* **2005**, 122.
(51) arthasarathi, R.; Subramanian, V.; Sathyamurthy, N. *J. Phys. Chem. A* **2006**, *110*, 3349–3351.
(52) Robertazzi, A.; Platts, J. A. *J. Phys. Chem. A* **2006**, *110*, 3992–4000.
(53) aller, M. P.; Robertazzi, A.; Platts, J. A.; Hibbs, D. E.; Williams, P. A. *J. Comput. Chem.* **2006**, *27*, 491–504.
(54) Moa, M. J. G.; Mandado, M.; Mosquera, R. A. *J. Phys. Chem. A* **2007**, *111*, 1998–2001.
(55) Parthasarathi, R.; Raman, S. S.; Subramanian, V.; Ramasami, T. *J. Phys. Chem. A* **2007**, *111*, 7141–7148.
(56) Vener, M. V.; Egorova, A. N.; Fomin, D. P.; Tsirelson, V. G. *Chem. Phys. Lett.* **2007**, *440*, 279–285.
(57) Keefe, C. D.; Isenor, M. *J. Phys. Chem. A* **2008**, *112*, 3127–3132.
(58) Suresh, C. H.; Mohan, N.; Vijayalakshmi, K. P.; George, R.; Mathew, J. M. *J. Comput. Chem.* **2009**, *30*, 1392–1404.
(59) Yau, A. D.; Byrd, E. F. C.; Rice, B. M. *J. Phys. Chem. A* **2009**, *113*, 6166–6171.
(60) Ebrahimi, A.; Khorassani, S. M. H.; Delarami, H. *Chem. Phys.* **2009**, *365*, 18–23.
(61) Nakanishi, W.; Hayashi, S.; Narahara, K. *J. Phys. Chem. A* **2008**, *112*, 13593–13599.
(62) Nakanishi, W.; Hayashi, S.; Narahara, K. *J. Phys. Chem. A* **2009**, *113*, 10050–10057.
(63) Mohajeri, A.; Karimi, E. *J. Mol. Struct. (Theochem)* **2006**, *774*, 71–76.
(64) Boyd, R. J.; Choi, S. C. *Chem. Phys. Lett.* **1985**, *120*, 80–85.
(65) Grabowski, S. J.; Sokalski, W. A.; Leszczynski, J. *J. Phys. Chem. A* **2005**, *109*, 4331–4341.
(66) Boys, S. F.; Bernardi, F. *Mol. Phys.* **1970**, *19*, 553–566.
(67) Hobza, P.; Sponer, J. *Chem. Rev.* **1999**, *99*, 3247–3276.
(68) Sponer, J.; Leszczynski, J.; Hobza, P. *J. Mol. Struct. (Theochem)* **2001**, *573*, 43–53.
(69) Sponer, J.; Leszczynski, J.; Hobza, P. *Biopolymers* **2002**, *61*, 3–31.
(70) Frisch, M. J.; Trucks, G. W.; Schlegel, H. B.; Scuseria, G. E.; Robb, M. A.; Cheeseman, J. R.; Montgomery, J., J. A.; Vreven, T.; Kudin, K. N.; Burant, J. C.; Millam, J. M.; Iyengar, S. S.; Tomasi, J.; Barone, V.; Mennucci, B.; Cossi, M.; Scalmani, G.; Rega, N.; Petersson, G. A.; Nakatsuji, H.; Hada, M.; Ehara, M.; Toyota, K.; Fukuda, R.; Hasegawa, J.;

Ishida, M.; Nakajima, T.; Honda, Y.; Kitao, O.; Nakai, H.; Klene, M.; Li, X.; Knox, J. E.; Hratchian, H. P.; Cross, J. B.; Bakken, V.; Adamo, C.; Jaramillo, J.; Gomperts, R.; Stratmann, R. E.; Yazyev, O.; Austin, A. J.; Cammi, R.; Pomelli, C.; Ochterski, J. W.; Ayala, P. Y.; Morokuma, K.; Voth, G. A.; Salvador, P.; Dannenberg, J. J.; Zakrzewski, V. G.; Dapprich, S.; Daniels, A. D.; Strain, M. C.; Farkas, O.; Malick, D. K.; Rabuck, A. D.; Raghavachari, K.; Foresman, J. B.; Ortiz, J. V.; Cui, Q.; Baboul, A. G.; Clifford, S.; Cioslowski, J.; Stefanov, B. B.; Liu, G.; Liashenko, A.; Piskorz, P.; Komaromi, I.; Martin, R. L.; Fox, D. J.; Keith, T.; Al-Laham, M. A.; Peng, C. Y.; Nanayakkara, A.; Challacombe, M.; Gill, P. M. W.; Johnson, B.; Chen, W.; Wong, M. W.; Gonzalez, C.; Pople, J. A. *Gaussian 03, Revision D.02*; Gaussian, Inc.: Wallingford, CT, 2004.

(71) Frisch, M. J.; Trucks, G. W.; Schlegel, H. B.; Scuseria, G. E.; Robb, M. A.; Cheeseman, J. R.; Scalmani, G.; Barone, V.; Mennucci, B.; Petersson, G. A.; Nakatsuji, H.; Caricato, M.; Li, X.; Hratchian, H. P.; Izmaylov, A. F.; Bloino, J.; Zheng, G.; Sonnenberg, J. L.; Hada, M.; Ehara, M.; Toyota, K.; Fukuda, R.; Hasegawa, J.; Ishida, M.; Nakajima, T.; Honda, Y.; Kitao, O.; Nakai, H.; Vreven, T.; Jr., J. A. M.; Peralta, J. E.; Ogliaro, F.; Bearpark, M.; Heyd, J. J.; Brothers, E.; Kudin, K. N.; Staroverov, V. N.; Kobayashi, R.; Normand, J.; Raghavachari, K.; Rendell, A.; Burant, J. C.; Iyengar, S. S.; Tomasi, J.; Cossi, M.; Rega, N.; Millam, J. M.; Klene, M.; Knox, J. E.; Cross, J. B.; Bakken, V.; Adamo, C.; Jaramillo, J.; Gomperts, R.; Stratmann, R. E.; Yazyev, O.; Austin, A. J.; Cammi, R.; Pomelli, C.; Ochterski, J. W.; Martin, R. L.; Morokuma, K.; Zakrzewski, V. G.; Voth, G. A.; Salvador, P.; Dannenberg, J. J.; Dapprich, S.; Daniels, A. D.; Farkas, O.; Foresman, J. B.; Ortiz, J. V.; Cioslowski, J.; Fox, D. J. *Gaussian 09, Revision A.02*; Gaussian, Inc.: Wallingford, CT, 2009.

(72) Keith, T. A. AIMAll, Version 08.09.20; aim.tkgristmill.com, 2009.

(73) Biegler-Konig, F. W.; Schonbohm, J. AIM2000, Version 2.0; AIM2000.de, 2002.

JP911990G